



# Modal tracking under large environmental influence

Sérgio Pereira<sup>1</sup> · Filipe Magalhães<sup>1</sup> · Jorge P. Gomes<sup>2</sup> · Álvaro Cunha<sup>1</sup>

Received: 23 July 2021 / Revised: 21 October 2021 / Accepted: 24 October 2021 / Published online: 8 November 2021  
© Springer-Verlag GmbH Germany, part of Springer Nature 2021

## Abstract

The installation of vibration-based structural health-monitoring systems relying in the study of natural frequencies to assess the condition of civil engineering structures is becoming more and more common. The extraction of these monitoring features can be achieved through automated operational modal analysis, combining output-only identification methods with cluster analyses, and comparing the identified modal properties with references, in a process known as modal tracking. However, changing environmental and operational conditions affect the dynamic behaviour of structures, disturbing the process of modal tracking, which may lead to the loss of important information and to misidentifications. In this context, this paper proposes a new methodology for modal tracking within the scope of automated operational modal analysis, especially prepared for scenarios with strong external influence on modal properties. A concrete arch dam with large variations of some natural frequencies is used as case study, and the proposed methodology is compared to a standard procedure using a quite unique monitoring data set continuously collected for 3 years.

**Keywords** Vibration-based monitoring · Operational modal analysis · Operational and environmental effects · Modal tracking · Dam monitoring

## 1 Introduction

Structural Health Monitoring (SHM) is an established research field addressing the main issues related to the study of civil engineering structures and their condition through the analysis of numerical and data-driven models [1, 2]. Many different monitoring systems considering real-time data have been implemented in quite many different types of structures through the years, from bridges to buildings or towers [3–5], to better understand structures and how to model them, but also to study how their behaviour evolves under varying conditions [6, 7] and their state deteriorates over time [8].

More specifically, vibration-based monitoring systems take advantage from structural vibrations due to ambient excitation, allowing to characterize the behaviour of a

structure under normal operating conditions. Nevertheless, since the time-series of accelerations recorded in situ are dependent not only on the structure they are measured, but also on the excitation that originates them, they by themselves do not constitute an interesting monitoring feature. Therefore, vibration-based health monitoring is commonly associated with automated operational modal analysis [9, 10], allowing to continuously identify the structure's modal properties, which are then used as monitoring features to evaluate the structures health condition evolution over time and the eventual emergence of a novel structural behaviour [11–14].

However, the automation of operational modal analysis involves many processing steps where errors and the loss of valuable information can occur and be propagated [15–17]. One of the most important and challenging steps consists in the sequential assignment of estimated modal properties to a particular vibration mode, a process known as modal tracking, which is commonly achieved through the comparison between the estimated natural frequencies and mode shapes with reference modal properties characteristic of a determined mode.

Effective procedures for modal tracking have been developed in the past and validated with experimental applications

---

✉ Sérgio Pereira  
sbp@fe.up.pt

<sup>1</sup> Construct-ViBest, Faculty of Engineering (FEUP),  
University of Porto, Rua Dr. Roberto Frias, 4200-465 Porto,  
Portugal

<sup>2</sup> National Laboratory for Civil Engineering (LNEC), Av. do  
Brasil 101, 1700-066 Lisbon, Portugal

[13, 18–20]. Although, with scenarios when environmental and operational conditions strongly and suddenly affect modal properties, including natural frequencies and mode shape complexity, classical procedures may struggle to present satisfactory results. In this context, this paper proposes a new methodology for modal tracking within the scope of automated operational modal analysis, especially prepared for scenarios with strong and sudden external influence on modal properties. A concrete arch dam with large variations of some natural frequencies is used as case study, and the proposed methodology is compared to a standard procedure using data from 3 years of continuous monitoring. Examples of other methodologies exploring the use of dynamic references and thresholds can be found in [21–23].

The standard procedure for modal tracking and the proposed methodology are presented in Sect. 2. The case study used to validate the new methodology is presented in Sect. 3, where the modal properties of the structure and the conditions affecting them are shown. Finally, the main results and validation of the methodology are presented in Sect. 4.

The main contributions of the paper consist in the methodology for modal tracking that is proposed and validated, in the presentation of an effective application of vibration-based monitoring of a concrete arch dam during three years, which is still uncommon in this type of structures [24], though a few applications have been developed in the recent past [25–28], and on the report of quite unique natural frequencies variations mainly motivated by the reservoir water level variations.

## 2 Tools used for automated operational modal analysis

### 2.1 Standard procedure for AOMA

Automated operational modal analysis (AOMA) [15] is used to continuously estimate the modal properties (natural frequencies, damping ratios, mode shapes) of a structure over a

period, with the minimum human intervention possible. The procedure consists in the successive application of operational modal analysis algorithms to groups of time-series of accelerations acquired on site over time, resulting in the continuous characterization of structural dynamic behaviour through different sets of modal properties obtained for each period analysed. These data can be processed in real time, as soon as the time-series are acquired, or later.

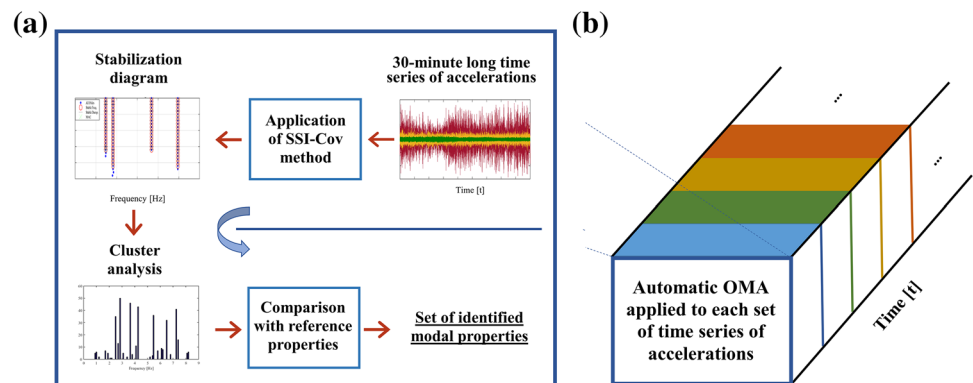
The procedure for automated operational modal analysis described in [29] has been widely adopted by the scientific community and used successfully in quite different applications [13, 19, 30–32]. In short, it develops as follows:

- (S1) definition of a set of reference modal properties (using ambient/forced vibration tests or numerical models);
- (S2) selection of a group of time series measured by the monitoring system during a defined period  $t$  (e.g.  $t = 30$  min);
- (S3) application of a parametric output-only identification method to the time series selected in (S2) using models of several orders;
- (S4) elimination of unstable poles after the application of stabilization criteria;
- (S5) performance of cluster analysis to group poles from different model orders representing the same mode;
- (S6) modal tracking of the structure's modal properties through the comparison between the clusters obtained in the previous point and the reference properties defined in (S1);
- (S7) selection of the next group of time series and repetition of the cycle from (S3) to (S7).

To complement the previous description, a schematic representation of the methodology is presented in Fig. 1.

The comparison performed in step (S6) between identified (pole,  $i$ ) and reference modal properties (ref,  $k$ —reference of mode  $k$ ) comprises two conditions related to the similarity between natural frequencies and mode

**Fig. 1** Standard procedure for automated operational modal analysis [27]



shapes. Moreover, identified poles are only associated with a vibration mode if both the following conditions are verified:

$$\text{abs} \left( \frac{f_{\text{pole},i} - f_{\text{ref},k}}{f_{\text{pole}}} \right) \times 100 < f_{\text{range}} [\%], \tag{1}$$

$$\text{MAC} (\text{modeshape}_{\text{pole},i}, \text{modeshape}_{\text{ref},k}) > \text{limit}_{\text{MAC}}, \tag{2}$$

where  $f_{\text{ref},k}$  and  $f_{\text{pole},i}$  represent the reference natural frequency of mode  $k$  and that of the evaluated pole  $i$ , while  $\text{modeshape}_{\text{ref},k}$  and  $\text{modeshape}_{\text{pole},i}$  represent vectors containing the modal ordinates of the reference mode shape of mode  $k$  and the one from the evaluated pole  $i$ . The definition of  $f_{\text{range}}$  should consider that structures are subjected to changing operational and environmental conditions that affect their dynamic behaviour throughout the year, therefore it is common for this limit to assume values between 5 and 10%. On the other hand, the modal assurance criterion (MAC) [33], defined in Eq. (3), is widely used as a mean to measure the similarity between two mode shapes, varying from 0 (completely distinct mode shapes) to 1 (directly proportional mode shapes). Values between 0.8 and 0.95 are commonly accepted for  $\text{limit}_{\text{MAC}}$ .

$$\text{MAC}(u_1, u_2) = \frac{\left( |u_1^T u_2| \right)^2}{\left( |u_1^T u_1| \right) \left( |u_2^T u_2| \right)}. \tag{3}$$

### 2.2 Proposed methodology

In the standard procedure for automated operational modal analysis presented in the previous section a single set of modal properties is used as reference, consisting of one value of frequency and a vector of modal ordinates for each vibration mode. However, in applications where operational and environmental conditions strongly affect the modal properties of the structure, it will be necessary to account for the variability due to these external conditions, guaranteeing no true estimates are being left out of the modal tracking ranges. Therefore, a choice arises between using tighter limits ( $f_{\text{range}}$  and  $\text{limit}_{\text{MAC}}$ ) in step (S6), losing valuable information, or using looser limits, which may lead to considerable numbers of misidentifications.

In this sense, it is proposed to substitute the fixed set of reference modal properties for a moving set of references using information from previous identifications and the measurement of external conditions.

To obtain the set of moving reference natural frequencies, the following new procedure is proposed:

- (N1) application of the standard procedure to a batch of data from a period large enough to conveniently characterize the environmental conditions affecting the structure, using loose limits in step (S6);
- (N2) definition of a multiple linear regression model between the natural frequencies identified with the standard procedure and variables representing the external conditions affecting the structure;
- (N3) definition of a vector of frequency references for each vibration mode, using the regression model built in (N2);
- (N4) application of standard procedure substituting the fixed frequency references by the new moving ones, according to the external conditions verified during the period under analysis.

Additionally, for each vibration mode, a matrix of  $r + 1$  reference mode shapes is used, including the original fixed reference and the mode shapes of the  $r$  previous identified poles. Equations (1) and (2) are then substituted by Eqs. (4) and (5):

$$\text{abs} \left( \frac{f_{\text{pole},i} - f_{\text{ref},k,\text{reg}}}{f_{\text{pole},i}} \right) \times 100 < f_{\text{range}} [\%], \tag{4}$$

$$\max \{ \text{MACX}(\text{modeshape}_{\text{pole},i}, \text{modeshape}_{\text{ref},k,r+1,}) \} > \text{limit}_{\text{MAC}}, \tag{5}$$

where  $f_{\text{ref},k,\text{reg}}$  represents the frequency reference obtained from the regression model, for each mode  $k$ , and  $\text{modeshape}_{\text{ref},k,r+1}$  represents each of the  $r + 1$  reference mode shapes associated with each vibration mode  $k$  at a certain time. A scheme of the procedure to update reference mode shapes during modal tracking is presented in Fig. 2. In this work a value of  $r$  equal to 5 is adopted.

Moreover, the calculation of the value of MAC is substituted by an extended version (MACX), suited to deal with complex vibration modes. This extended version is presented in Eq. (6), as proposed by [34], and it has the particularity of becoming the same as the original MAC when purely real modes are at stake.

$$\text{MACX}(u_1, u_2) = \frac{\left( |u_1^* u_2| + |u_1^T u_2| \right)^2}{\left( |u_1^* u_1| + |u_1^T u_1| \right) \left( |u_2^* u_2| + |u_2^T u_2| \right)}. \tag{6}$$

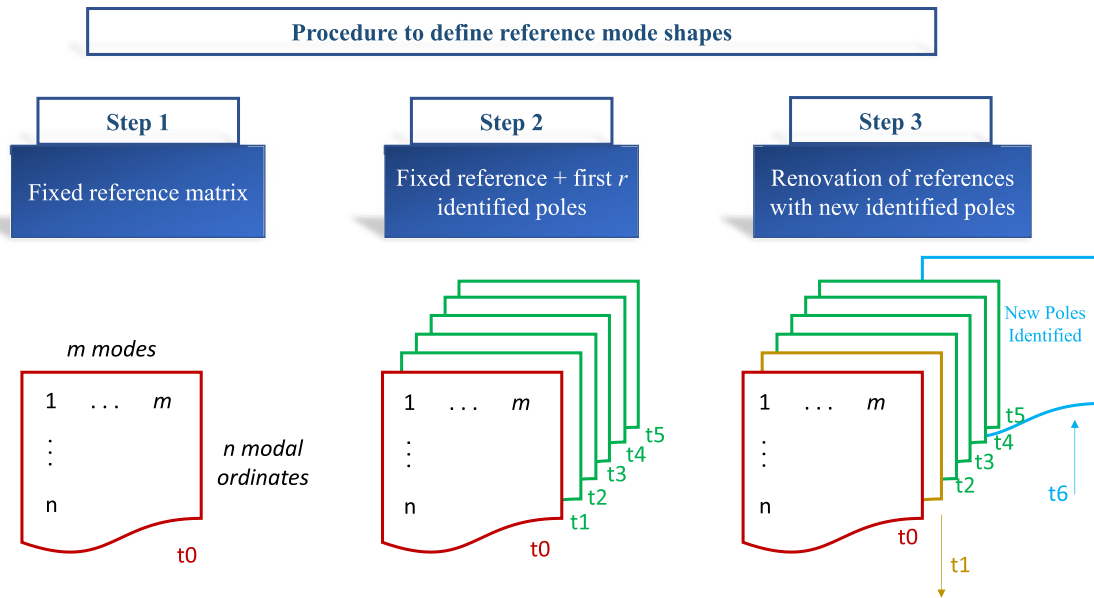


Fig. 2 Procedure to define reference mode shapes

### 3 Foz Tua dam

#### 3.1 Description of dam and monitoring system

The Foz Tua hydroelectric development is located in the north of Portugal and it is constituted by a power plant installed with 270 MW of power capacity and by a 108 m high, double-curvature concrete arch dam, whose construction was concluded by the end of 2016. The 275 m long arch (crest length) is composed of 18 concrete blocks, separated by vertical contraction joints, and includes six visit galleries at different levels. The full storage level is at 172 m. Figure 1a shows a picture of the dam and its reservoir dated November 2016, before the start of the exploration period.

The dam has been equipped with a vibration-based structural health-monitoring system composed primarily of 12 uniaxial, force-balance accelerometers that were radially disposed over the first two visit galleries, attending to the results of forced vibrations tests and the analysis of a numerical model of the structure. Four accelerometers are in the upper visit gallery (GV1), divided by the two sides of the dam's spillway gates, and the other eight accelerometers are in the second visit gallery (GV2). All the accelerometers are configured to measure in the range  $-0.25\text{ g}/+0.25\text{ g}$  and connected to a set of digitizers, being the synchronization of the data accomplished by GPS.

The position of the accelerometers is characterized in Fig. 3b by blue dots in a scheme of the dam. There is one extra accelerometer positioned in the left side of the structure, which is not entirely symmetric. The continuous

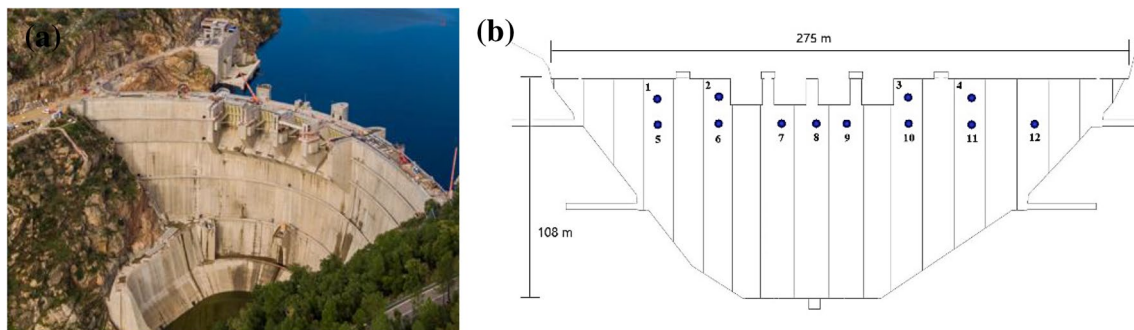


Fig. 3 Foz Tua dam: **a** aerial view [35]; **b** disposition of accelerometers

dynamic monitoring system is configured to record 30-min-long time series of accelerations, though this length can be adjusted if necessary.

### 3.2 Vibration levels

Concrete dams are generally located in remote places, apart from intense human activity, and therefore subjected to very low intensity excitations, of the order of just a few micro  $g$  [36], which poses a challenge to the performance of vibration-based structural health monitoring. This excitation is due to the natural conditions in their surroundings, such as the effect of the wind, the occurrence of small seismicity and wildlife activity, as well as to human related affairs such as the eventual passage of nearby road/rail traffic and the normal daily operation of the structure.

In the case of Foz Tua dam, no excitation is purposely applied in the structure with the intention of performing modal identification and the prevalent source of excitation is due to the electricity production operations in the nearby power plant, when it is active. Maximum accelerations, and their root mean square (RMS), were determined for each 30-min-long time series to characterize the magnitude of the vibration levels verified in the structure during the continuous monitoring. This characterization is presented in Fig. 4 for the period between January 20 and February 10, 2018, where each colour corresponds to a different accelerometer.

- a first stage on the left part of each figure, when higher vibration levels with clear differentiation between accelerometers occur, indicating an uninterrupted operation of the power plant.
- a second stage on the right part of each figure, when much lower vibration levels are recorded along with sparsely distributed higher accelerations, suggesting pure ambient vibration as source of structural excitation during most of the presented setups.

Though higher vibration levels occur when the power plant is operating, it is worth noting that in this scenario, the turbine rotation frequency (185.5 r.p.m.  $\sim$  3.09 Hz) pollutes the time series of accelerations, becoming a source of misidentifications during the process of modal tracking. The strategy presented in [37] is used to minimize this parasite effect, consisting of the elimination of poles with frequency equal to 3.09 Hz and damping below 0.4%.

### 3.3 Modal properties of the structure

The covariance-driven stochastic subspace identification method (SSI-Cov) [38] was used on 30-min long time series of accelerations with a sampling frequency of 25 Hz to identify the modal properties of the structure, after application of eighth-order low-pass Butterworth filtering [39] with a cut frequency of 8.5 Hz. Model orders between 2 and 150 were considered along with maximum lags of the correlation functions equal to 50 points, having in mind state-of-the-art recommendations [40] and tuning of the algorithm in some relevant setups.

The first five vibration modes were identified from time-series recorded on December 8th, the first day of monitoring, and the natural frequencies, damping values and modal configurations obtained are presented in Table 1. The first five vibration modes can be found between 3 and 7 Hz, with damping values between 1 and 1.5%. A three-dimensional representation of the modal configurations is presented in Fig. 5, where the modal ordinates are represented with blue dots and the full modal configurations were obtained using

**Table 1** Modal properties of Foz Tua dam—08/12/2017

Mode	Frequency (Hz)	Damping (%)	Description
1	3.03	0.95	Antisymmetric
2	3.26	1.47	Symmetric
3	4.19	1.37	Symmetric
4	5.61	1.36	Antisymmetric
5	6.72	1.98	Symmetric

**Fig. 4** Maxima and RMS accelerations measured between 20/01/2018 and 0/02/2018

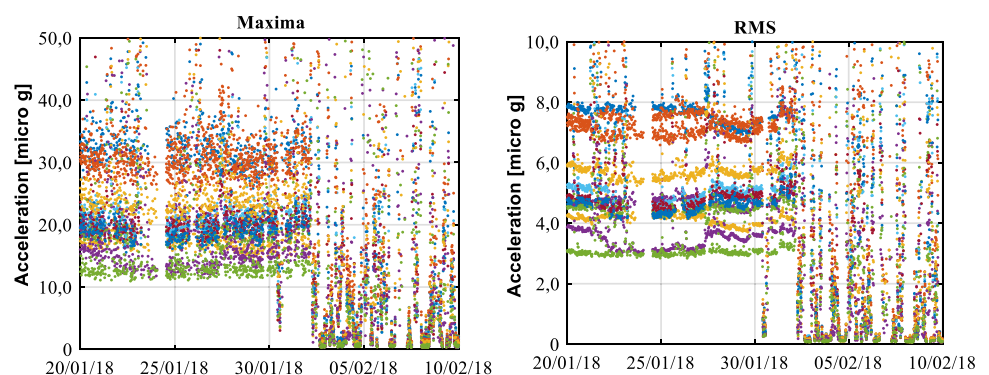
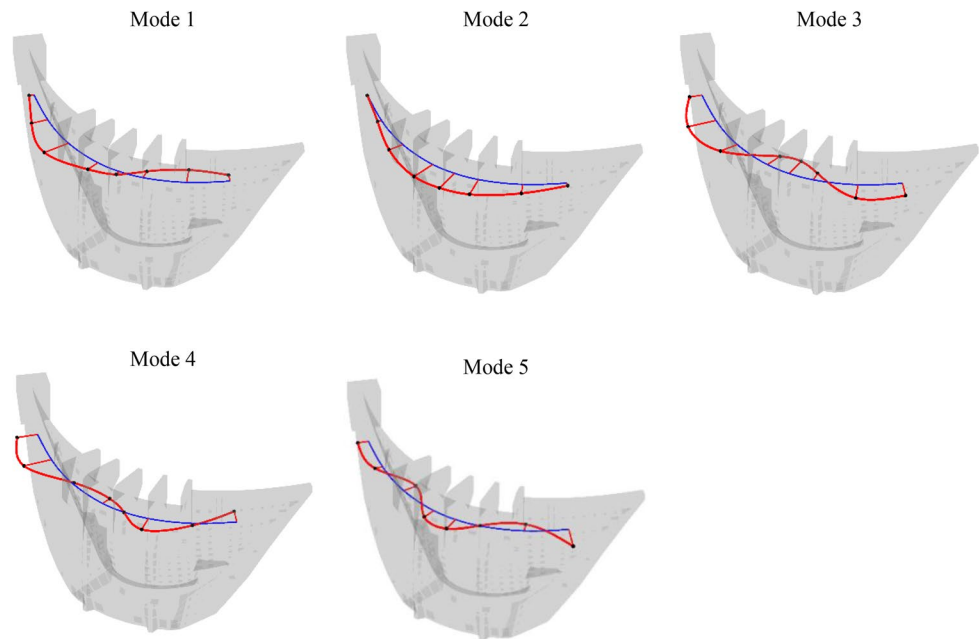


**Fig. 5** Modal ordinates of the first five vibration modes of Foz Tua arch dam at instrumented points



interpolations. This representation considers only the results from accelerometers located from position 5–12 (see Fig. 3) with purpose of favouring the distinction between symmetrical and anti-symmetrical shapes. In this case, the first and fourth modes are anti-symmetrical and the second, third, and fifth present symmetrical mode shapes. The identification of other modes, even though possible, is conditioned by the number of sensors available in the same horizontal alignment (GV2), making it harder to correctly identify the mode shape of superior mode orders.

The modal properties here presented are used as fixed references in the automated operational modal analysis presented in the next section.

### 3.4 Preliminary analysis of natural frequencies variations

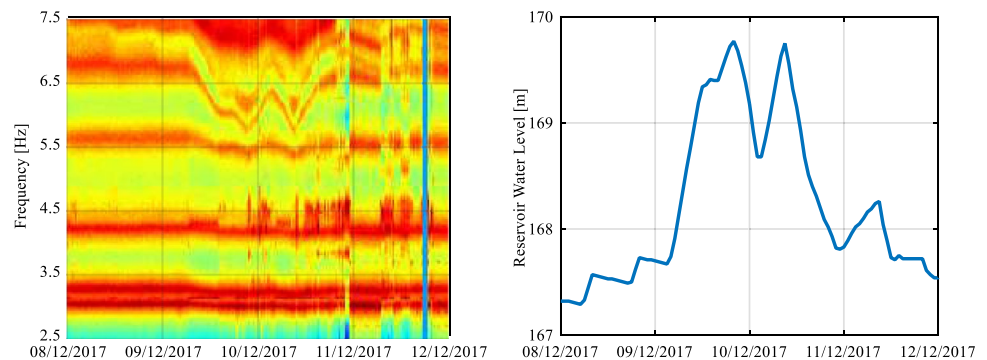
A straightforward method to perform a preliminary analysis on the evolution of natural frequencies consists of the application of the singular value decomposition to each time

series of acceleration and the assembly of the sample's spectra first singular values, allowing the construction of a colour map. In this type of figures, colours are functions of intensity, with warm colours (red) associated with more energy in the respective frequency bands. Therefore, approximate estimates of the natural frequencies of the structure are indicated by red zones.

A colour map with the evolution of natural frequencies for four days is presented in the left part of Fig. 6. It is possible to differentiate four red horizontal alignments between 3 and 6 Hz, which corresponds to the first four vibrations modes, and a fifth alignment showing important variations, which corresponds to the fifth mode.

The shape of the frequency variations presented by the fifth mode follows the inverse shape of the evolution of the water level of the reservoir in the same period, which is presented in the right part of Fig. 6. Such a similarity suggests a strong influence of this operational condition on the modal properties of the structure, in accordance with the results presented by previous works on the monitoring of concrete

**Fig. 6** On the left: colour map of natural frequencies; on the right: reservoir water level



dams [25, 41]. It is worth noticing, though, that in the case of Foz Tua dam this effect seems to be unusually preponderant, since variations of less than 3 m in the level of water in the reservoir led to variations of almost 1 Hz in the natural frequency of the fifth vibration mode.

## 4 Results

### 4.1 Validation of the proposed methodology

The standard AOMA procedure described in Sect. 2 was used to identify and track the modal properties of Foz Tua dam first five modes of vibration for 3 years. The natural frequencies and mode shapes presented in Table 1 and Fig. 5 were used as fixed references and the values adopted for  $f_{\text{range}}$  and  $\text{limit}_{\text{MAC}}$  were, respectively, 10% and 0.85.

The success rates for the identification of the first five vibration modes, between 01/01/2018 and 31/12/2020, using the standard procedure are presented in Table 3 (“previous success rate”). Though the first three modes of vibration were tracked in more than 70% of the analysed setups, modes 4 and 5 could not be tracked in more than half of the setups.

To improve the results, the new methodology proposed in Sect. 2 is applied. First, a multiple linear regression model is built having in mind the case study presented in [27].

One year of data measured during 2018 was used to train the model, consisting of the following variables:

- Natural frequencies identified with the standard procedure;
- Reservoir water level (see Fig. 7);
- The square values of the reservoir water level;
- Ambient temperature (see Fig. 8);
- 2-day moving average of ambient temperature, to account for thermal inertia in concrete.

Observing Fig. 7, it becomes clear that during the year of 2018, the level of water in the reservoir varies only between 166.5 and 170 m but presenting sudden variations. On the other hand, the ambient temperature evolution presented in Fig. 8 shows clear daily oscillations and the expected seasonal wave.

Different vibration modes are dominated by different external conditions. This is clear through the analysis of Fig. 9 where the frequencies of the first and fifth modes are represented together with the external effect dominating their variations, temperature and reservoir water level, respectively.

The multiple linear regression models built for each vibration mode present a strong ability to predict the

**Fig. 7** Evolution of reservoir water level (above sea level) during 2018

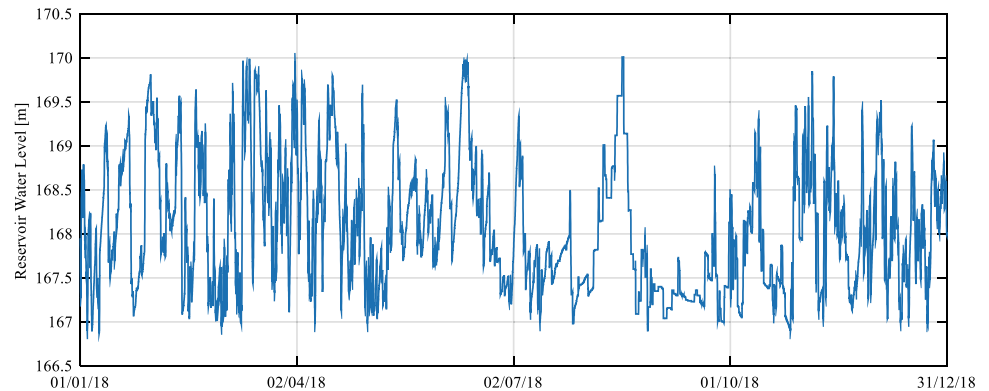
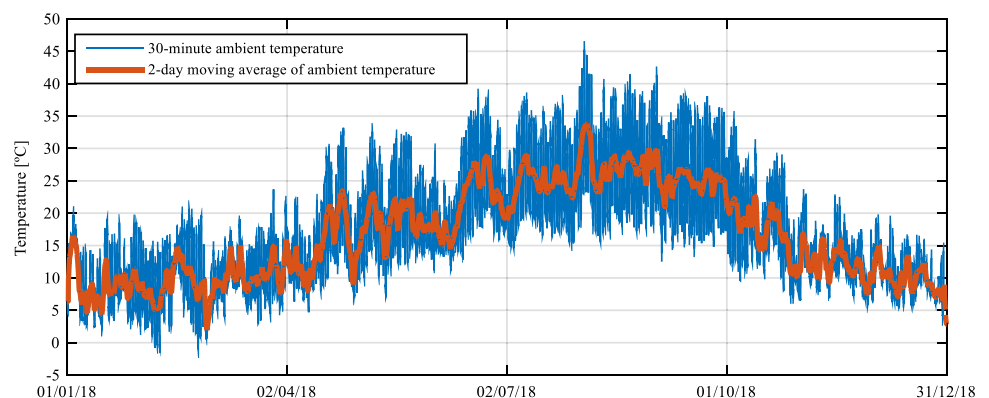


**Fig. 8** Evolution of ambient temperature and respective 2-day moving average during 2018



values of natural frequencies at a certain moment, as shown by the coefficients of determination presented in Table 2, with values equal or above 0.85. The coefficients related with each variable composing the regression models are also presented in this table. Adding coefficients of variables related with water level and temperature, a relative preponderance of each effect is obtained for each vibration mode.

The process of modal tracking was then repeated, now considering the moving frequency references obtained from the application of the regression models, and the moving mode shape references as defined by Eq. 5. Additionally, MACX was used to compute the similarity between mode shapes and the values adopted for  $f_{range}$  and  $limit_{MAC}$  were, respectively, 5% and 0.85.

The evolution of tracked natural frequencies is presented in Fig. 10, where each point represents a 30-min estimate. The observation of the evolution of natural frequencies suggests that the first four modes are mostly affected by the seasonal thermal wave, while the behaviour of the fifth mode is dominated by the variations in the level of water in the reservoir.

The success rates for the modal tracking using the proposed methodology are presented in Table 3, along with the statistical characterization of natural frequencies and damping values. All success rates increased comparatively to the application of the standard methodology, with special emphasis to the cases of modes 4 and 5 which doubled the number of tracked estimates. The unusual variability of the fifth mode natural frequency is also defined by

**Fig. 9** Relation between natural frequencies and respective dominant external effects

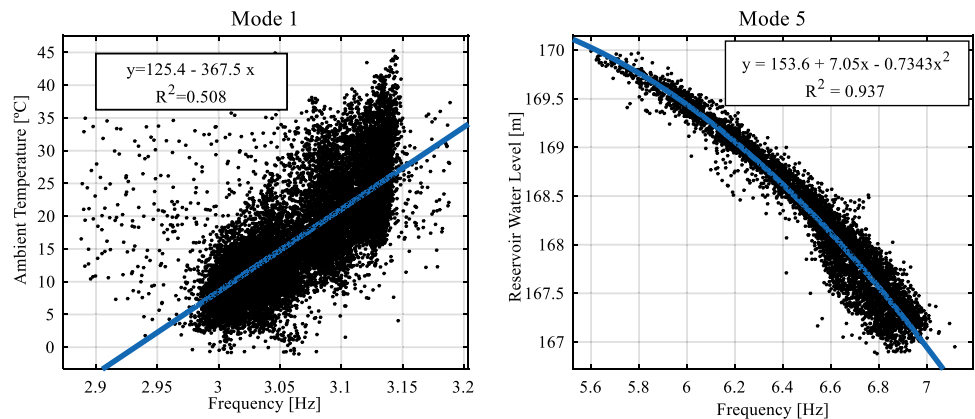
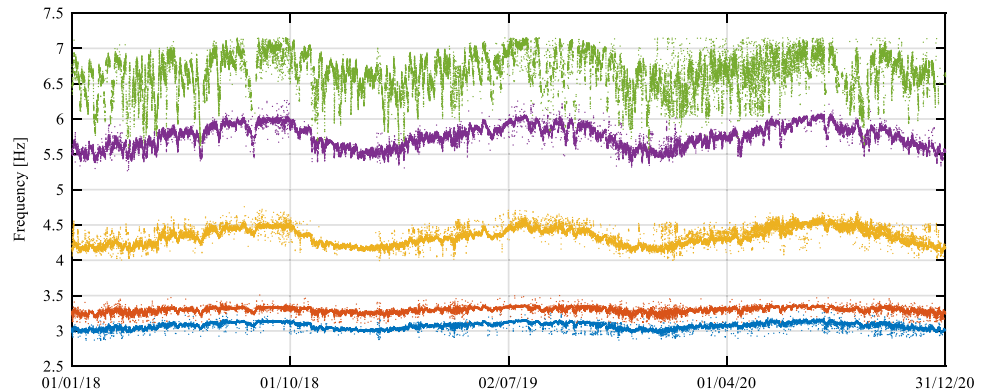


**Table 2** Multiple linear regression model: coefficients of determination

	Mode	1	2	3	4	5
Linear regression coefficients	Coefficient of determination $R^2$	0.88	0.85	0.88	0.89	0.96
	Intercept	3.068	3.287	4.310	5.730	6.631
	Water level	-0.283	0.239	-1.119	3.943	6.000
	Squared water level	0.266	-0.261	1.089	-4.016	-6.257
	Ambient temperature	0.0043	0.0051	0.0091	0.0127	0.0287
	2-day temperature average	0.0317	0.0155	0.0874	0.1149	0.0313

**Fig. 10** Evolution of natural frequencies between 01/01/2018 and 31/12/2020





the abnormally high value of its standard deviation ( $f_{std}$ ), which is equal to 0.276 Hz.

A 6-week zoom of the tracked natural frequencies is presented in Fig. 11 using black points, which are overlapped with the colourmap obtained with singular value decomposition for the same period, showing a synchronous evolution of the natural frequencies with the hotter lines of the map. On the one hand, Fig. 11 proves the tracked frequencies follow the real evolution of the natural frequencies and not just the trend provided by the regression models used to predict the best possible frequency references. On the other hand, the few outliers that can be found throughout the figure prove that the tracking algorithm does not force any specific path and that random variability is still permitted. Anyhow, it would be possible to reduce even more the number of outliers decreasing the value of  $f_{range}$ .

Finally, dashed lines are used in Fig. 11 to point local maxima (dark blue) and minima (light blue) of reservoir water levels, which are in all cases close to global extreme values. The mode shapes obtained for modes 1 and 5 in these setups are presented in Fig. 12, using corresponding colours. Through the analysis of the two figures, it becomes clear that water level has a strong effect on the mode shape of mode 5, but limited influence on the mode shape of mode 1.

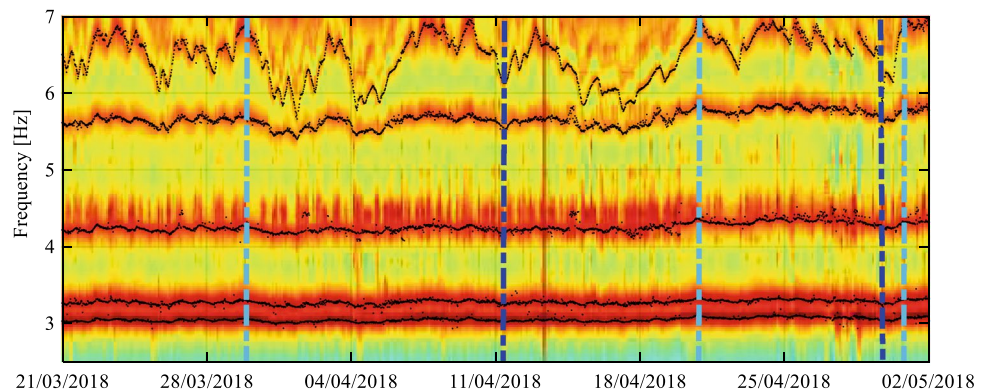
### 4.2 Additional considerations on the effect of water level

It was shown before that the variations in the reservoir water level have a strong effect not only on the fifth mode natural frequency, but on its mode shape as well. This is clear through the observation of Fig. 12, where mode shapes are presented for extreme values of water level. Additionally,

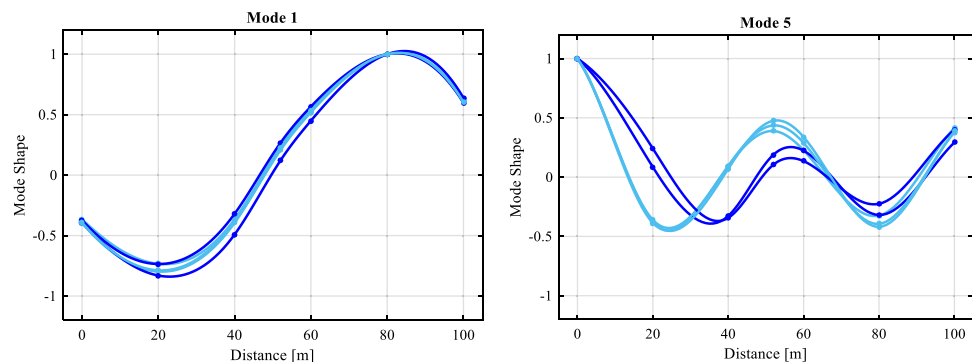
**Table 3** Characterization of the tracked modal properties between 01/01/2018 and 31/12/2020, using the proposed methodology

Mode	Previous success rate (%)	New success rate (%)	$f_{mean}$ (Hz)	$f_{std}$ (Hz)	$\xi_{mean}$ (%)	$\xi_{std}$ (%)
1	86.9	95.5	3.07	0.046	1.02	0.345
2	98.5	99.2	3.29	0.039	1.29	0.326
3	69.0	93.8	4.33	0.120	1.43	0.353
4	44.6	93.3	5.75	0.159	1.32	0.311
5	36.9	80.7	6.64	0.276	1.26	0.496

**Fig. 11** 6-week evolution of tracked natural frequencies



**Fig. 12** Mode shapes of modes 1 and 5 at points defined in Fig. 11, corresponding to maximum and minimum values of reservoir water level



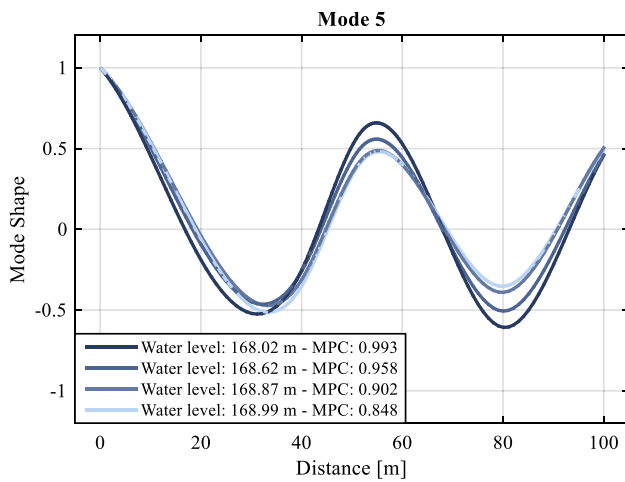


**Fig. 13** Mode shape of the fifth vibration mode for increasing values of water levels

the mode shapes of the fifth vibration mode are presented in Fig. 13 for four water level scenarios identified between the 1st and 2nd of January 2019, gradually increasing from 168 and 169 m, showing that the mode shape variation progressively follows the increase in the level of water.

Additionally, the modal phase collinearity (MPC) [42], a measure of the level of complexity of a mode shape,

decreases from 0.993 to 0.848 in the same period, suggesting variations in water level are affecting mode complexity as well. In this context, a comparison between the evolution of water level and the MPC of the fifth mode for 10 days is presented in Fig. 14, showing an inverse correlation between the two variables, since the values of MPC decrease when the level of water in the reservoir increases, and vice versa. Finally, Fig. 15 presents the evolution of the MACX of mode 5 relative to the fix reference, during the same period, showing once more the effects of water level in this mode shape.

These results support the need for the use of moving mode shape references (as proposed in Eq. 5) and for the comparison between mode shapes using the extended version of the modal assurance criterion (MACX).

### 5 Conclusion

A new methodology for modal tracking within the scope of automated operational modal analysis was proposed with the intention of improving the outcomes of the current standard procedure. The proposed methodology is especially prepared to deal with extreme and sudden modal variability due to the effects of environmental and operational conditions and with complex vibration modes.

**Fig. 14** Comparison between the variation of the level of water in the reservoir and the modal phase collinearity of the fifth mode shape. Water level axis in reversed for comparison purposes

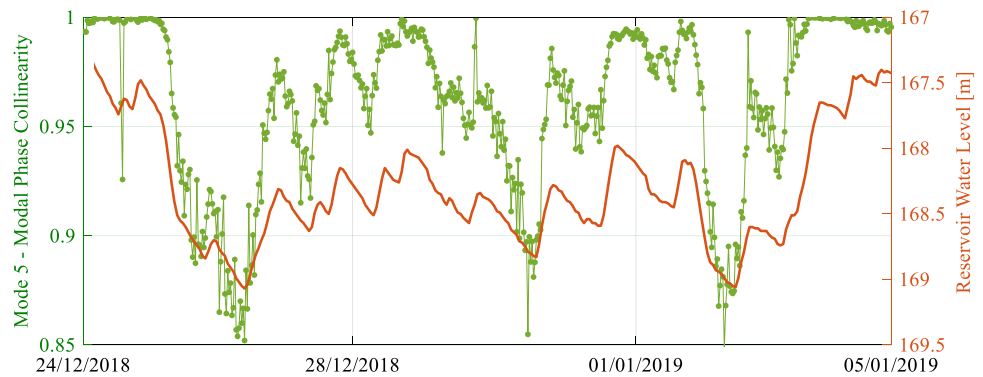
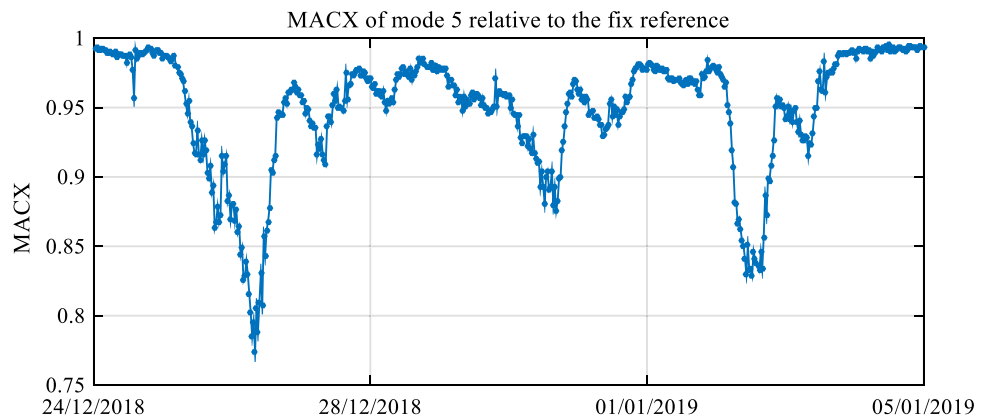


**Fig. 15** Comparison of the evolution of MACX of mode 5 relative to the fix reference



The vibration-based monitoring of a concrete arch dam for three years was presented as case study and used to validate the proposed methodology through the comparison between results obtained with it and with a standard procedure. It was possible to considerably improve the success rates in modal tracking using the methodology proposed, especially for the vibration modes that are more affected by external conditions.

The studied arch dam shows a quite unique behaviour, with different vibration modes being primarily affected by different external conditions. The behaviour of the dam's fifth vibration mode is particularly peculiar, presenting frequency variations of more than 1 Hz in just a few hours, constituting a true challenge for modal tracking tools. This behaviour is clearly triggered by the effect of water level variations, which has impact on the total vibrating mass and on the hydrostatic pressure in the arch, leading to the partial closing and opening of the dam's contraction joints.

Though the proposed methodology is presently validated using data from an arch dam, it should be able to perform well also when applied in the monitoring of other types of structures, such as bridges and wind turbines. It presents the drawback of needing the a priori definition of the environmental and operational conditions affecting the structure and their use as input variables in the characterization of the regression models estimating frequency references.

In future research, the authors intend to compare the success rate of the methodology proposed with other methods using adaptive thresholds.

**Acknowledgements** This work was financially supported by national funds through the FCT/MCTES (PIDDAC), under the project PTDC/ECI-EST/29558/2017, and by Base Funding—UIDB/04708/2020 and Programmatic Funding—UIDP/04708/2020 of the CONSTRUCT—Instituto de I&D em Estruturas e Construções—also funded by national funds through the FCT/MCTES (PIDDAC). The authors would also like to thank the collaboration and support provided by EDP Produção and by Engie/Movhera.

## References

- Farrar CR, Worden K (1851) An introduction to structural health monitoring. *Philos Trans R Soc A Math Phys Eng Sci* 2007(365):303–315
- Brownjohn JMW (1851) Structural health monitoring of civil infrastructure. *Philos Trans R Soc A Math Phys Eng Sci* 2007(365):589–622
- Cross EJ, Koo KY, Brownjohn JMW, Worden K (2013) Long-term monitoring and data analysis of the Tamar Bridge. *Mech Syst Signal Process* 35(1–2):16–34
- Pallarés FJ, Betti M, Bartoli G, Pallarés L (2021) Structural health monitoring (SHM) and nondestructive testing (NDT) of slender masonry structures: a practical review. *Constr Build Mater* 297:123768
- Ubertini F, Cavalagli N, Kita A, Comanducci G (2018) Assessment of a monumental masonry bell-tower after 2016 Central Italy seismic sequence by long-term SHM. *Bull Earthq Eng* 16(2):775–801
- Deraemaeker A, Reynders E, De Roeck G, Kullaa J (2008) Vibration-based structural health monitoring using output-only measurements under changing environment. *Mech Syst Signal Process* 22(1):34–56
- Rainieri C, Notarangelo MA, Fabbrocino G (2020) Experiences of dynamic identification and monitoring of bridges in serviceability conditions and after hazardous events. *Infrastructures* 5(10):86
- García-Macías E, Ubertini F (2020) MOVA/MOSS: two integrated software solutions for comprehensive structural health monitoring of structures. *Mech Syst Signal Process* 143:106830
- Magalhães F, Cunha A (2011) Explaining operational modal analysis with data from an arch bridge. *Mech Syst Signal Process* 25(5):1431–1450
- Rainieri C, Fabbrocino G (2015) Development and validation of an automated operational modal analysis algorithm for vibration-based monitoring and tensile load estimation. *Mech Syst Signal Process* 60:512–534
- Salawu OS (1997) Detection of structural damage through changes in frequency: a review. *Eng Struct* 19(9):718–723
- Fan W, Qiao P (2011) Vibration-based damage identification methods: a review and comparative study. *Struct Health Monit* 10(1):83–111
- Magalhães F, Cunha A, Caetano E (2012) Vibration based structural health monitoring of an arch bridge: from automated OMA to damage detection. *Mech Syst Signal Process* 28:212–228
- Masciotta MG, Ramos LF, Lourenço PB, Vasta M (2017) Damage identification and seismic vulnerability assessment of a historic masonry chimney. *Ann Geophys* 60(4):S0442
- Reynders E, Houbrechts J, De Roeck G (2012) Fully automated (operational) modal analysis. *Mech Syst Signal Process* 29:228–250
- Pereira S, Reynders E, Magalhães F, Cunha Á, Gomes JP (2020) The role of modal parameters uncertainty estimation in automated modal identification, modal tracking and data normalization. *Eng Struct* 224:111208
- Neu E, Janser F, Khatibi AA, Orifici AC (2017) Fully automated operational modal analysis using multi-stage clustering. *Mech Syst Signal Process* 84:308–323
- Rainieri C, Fabbrocino G, Cosenza E (2011) Near real-time tracking of dynamic properties for standalone structural health monitoring systems. *Mech Syst Signal Process* 25(8):3010–3026
- Martins N, Caetano E, Diord S, Magalhães F, Cunha T (2014) Dynamic monitoring of a stadium suspension roof: wind and temperature influence on modal parameters and structural response. *Eng Struct* 59:80–94
- Maes K, Lombaert G (2021) Monitoring railway bridge KW51 before, during, and after retrofitting. *J Bridge Eng* 26(3):04721001
- Cabboi A, Magalhães F, Gentile C, Cunha Á (2017) Automated modal identification and tracking: application to an iron arch bridge. *Struct Control Health Monit* 24(1):e1854
- Zonno G, Aguilar R, Boroschek R, Lourenço PB (2021) Environmental and ambient vibration monitoring of historical adobe buildings: applications in emblematic Andean Churches. *Int J Archit Herit* 15(8):1113–1129
- Marrongelli G, Gentile C (2019) Development and application of automated OMA algorithms. In: 8th IOMAC—international operational modal analysis conference, proceedings
- Bukenya P, Moyo P, Beushausen H, Oosthuizen C (2014) Health monitoring of concrete dams: a literature review. *J Civ Struct Health Monit* 4(4):235–244
- Darbre GR, Proulx J (2002) Continuous ambient-vibration monitoring of the arch dam of Mauvoisin. *Earthq Eng Struct Dyn* 31(2):475–480

26. Oliveira S, Alegre A (2020) Seismic and structural health monitoring of Cabril dam. Software development for informed management. *J Civ Struct Health Monit* 10(5):913–925
27. Pereira S, Magalhães F, Gomes JP, Cunha Á, Lemos JV (2021) Vibration-based damage detection of a concrete arch dam. *Eng Struct* 235:112032
28. Liseikin A, Seleznev V, Adilov Z (2020) Monitoring of the natural frequencies of Chirkey arch dam. *Mag Civ Eng* 4:15–20
29. Magalhães F, Cunha A, Caetano E (2009) Online automatic identification of the modal parameters of a long span arch bridge. *Mech Syst Signal Process* 23(2):316–329
30. Ubertini F, Comanducci G, Cavalagli N (2016) Vibration-based structural health monitoring of a historic bell-tower using output-only measurements and multivariate statistical analysis. *Struct Health Monit* 15(4):438–457
31. Giordano PF, Ubertini F, Cavalagli N, Kita A, Masciotta MG (2020) Four years of structural health monitoring of the San Pietro bell tower in Perugia, Italy: two years before the earthquake versus two years after. *Int J Mason Res Innov* 5(4):445–467
32. Oliveira G, Magalhães F, Cunha Á, Caetano E (2018) Vibration-based damage detection in a wind turbine using 1 year of data. *Struct Control Health Monit* 25(11):e2238
33. Allemang RJ (2003) The modal assurance criterion—twenty years of use and abuse. *Sound Vib* 37(8):14–23
34. Vacher P, Jacquier B, Bucharles A (2010) Extensions of the MAC criterion to complex modes. In: *Proceedings of ISMA 2010—international conference on noise and vibration engineering, including USD 2010*
35. EDP. Energias de Portugal. [cited 2018 21/09/2018]. [http://www.a-nossa-energia.edp.pt/centros\\_produtores/](http://www.a-nossa-energia.edp.pt/centros_produtores/)
36. Pereira S, Magalhães F, Cunha Á, Moutinho C, Pacheco J (2021) Modal identification of concrete dams under natural excitation. *J Civ Struct Health Monit* 11(2):465–484
37. Pereira S, Magalhães F, Gomes JP, Cunha Á, Lemos JV (2018) Dynamic monitoring of a concrete arch dam during the first filling of the reservoir. *Eng Struct* 174:548–560
38. Peeters B (2000) System identification and damage detection in civil engineering. Katholieke Universiteit Leuven
39. Mathworks (2016) Matlab. R2016a
40. Li S, Wang JT, Jin AY, Luo GH (2020) Parametric analysis of SSI algorithm in modal identification of high arch dams. *Soil Dyn Earthq Eng* 129:105929
41. Mendes P (2010) Observação e análise do comportamento dinâmico de barragens de betão. 2010 Faculdade de Engenharia da Universidade do Porto
42. Pappa RS, Elliott KB, Schenk A (1993) Consistent-mode indicator for the eigensystem realization algorithm. *J Guid Control Dyn* 16(5):852–858

**Publisher's Note** Springer Nature remains neutral with regard to jurisdictional claims in published maps and institutional affiliations.